



Spectroscopic Studies of Dy³⁺ Ion Doped Molybdenum Bismuth Borate Glasses For Optical Application

Amal Metwally,^{1*} Mervat M. Abdel Aal,¹ Asmaa Ratep,¹ Ismail Kashif²

¹ Physics Department, Faculty of Women, Ain Shams University, Heliopolis, Cairo, 11757, Egypt

² Physics Department, Faculty of Science, Al-Azhar University, Nasr City, Cairo, 11651, Egypt



CrossMark

Abstract

A glass system 45B₂O₃-50 Bi₂O₃-5MoO₃ glass system containing various proportions of Dy₂O₃ was prepared by the conventional melt quenching technique. The density (ρ) and molar volume of the prepared glass is determined. The areas of BO₃ and BO₄ were obtained from the FTIR spectra deconvolution. The optical absorption and emission spectra have been systematically studied and discussed. Also using Judd-Ofelt parameters to study the local structure around Dy ions. The yellow to blue intensity ratio, (Commission Internationale de l'éclairage) CIE chromaticity diagram coordinates, and color temperature values correlated were also calculated using emission spectra to evaluate the emitted light. The results obtained indicate the usefulness of glass samples for potential white LED applications.

Keywords: Molybdenum bismuth borate glasses; optical absorption; optical emission; Judd-Ofelt parameters; optical application.

1. Introduction

A commercial white light-emitting diode (WLED) is obtained in two ways. The first method is to use InGaN LED and YAG: Ce³⁺ + emits blue light and yellow phosphor. The other way is to use a UV chip to come out of the RGB phosphor to produce white light [1][2]. These diodes are important solid-state light sources [3] [4] due to their pros, such as high brightness, low power consumption, and long time. It has many problems [1] [4] [5] [6] [7] [8], such as large amount of scattered light and low light extraction efficiency, low lifetime, low thermal stability, low intensity glossiness and high correlated color temperature (7750 K) which is complex and expensive. Otherwise, glasses doped with rare-earth ions with a specific composition are an alternative to Pc W-LEDs due to their advantages [6]. It saves electrical energy and reduces carbon emissions [1] [4] [8][9] [10] also has excellent chemical and thermal stability, low fabrication cost, and ease of forming any shape. The glasses doped with rare-earth ions form the basis of optical devices such as amplifiers, sensors, and lasers. It has good emission light in the visible, infrared, and near-infrared regions of the electromagnetic spectrum.

[11] [12] (Peng et al., 2020). (Dy³⁺) ion doped with glass composition is interesting because it absorbs low energy like UV or blue LED light [8][11] [15] mainly in the visible region, in the blue region of the spectrum (460–500 nm), and the yellow region (560–600 nm). The ratio between yellow and blue Y/B emission is an effective tool to probe the structural nature of the luminescent glass. The intensity of the Y/B emission depends only on the Dy³⁺ concentration and the type of host glasses. This ratio is an important parameter as it describes the chances of any transitions to occur via stimulated emission. [1][8][14][16][17][18][19]. The photoluminescence of Dy³⁺ doped borate glass was studied and concluded that, the borate glass sample contains 0.8 mol% Dy³⁺ has the highest luminescent intensity and is suitable for bright yellow light production [20]. V. Uma et al. [21] studied the structural and optical properties of lithium tellurofluoroborate glass samples doped with Dy³⁺ for white light applications and observed that, the electric dipole transition in luminescence spectra was predominant compared to the magnetic dipole transition, and found that the color coordinates of prepared glasses are found in the white light region.

*Corresponding author e-mail: Amal.ahmed@women.asu.edu.eg; (Amal Metwally).

Receive Date: 31 October 2021, Revise Date: 17 November 2021, Accept Date: 07 December 2021

DOI: 10.21608/EJCHEM.2021.103672.4799

©2022 National Information and Documentation Center (NIDOC)

Ramteke et al. [22] tested the physical and optical properties of lithium borosilicate glass doped with dysprosium ions, and the authors concluded that the increment of density and molar volume with the addition of Dy_2O_3 . Photometric studies have confirmed that this type of glass is likely suitable for white light applications. P. P. Pawar et al. [8] studied lithium borate glass samples containing Dy^{3+} ions content. It found that the stability of the glass and optical basicity increased as the optical band gap decreased with the increase of Dy^{3+} ions. The Photoluminescence (PL) emission spectra also show two intense blue and yellow bands and a weak red band. They found that the glass samples understudy useful in setting up pure white LEDs. Xin-Yuan Sun et al. [23] studied silicate glass doped varies concentrations of Dy^{3+} ions. It found that the optimum doping concentration of Dy^{3+} ions is 3.0 Wt% by weight. They found silicate glass is more convenient for generating the white light of blue LED chips.

The aim of this work is to focus on the preparation of modifier-free glass and study the effect of adding renewable energy on the composition and optical properties of glass samples.

2. Experimental work:

Glass sample composition $50\text{Bi}_2\text{O}_3$ - 5MoO_3 - $45\text{B}_2\text{O}_3$ - $x\text{Dy}_2\text{O}_3$ where $x=0.05, 0.1, 0.3, 0.5, 0.7, 1$ mol% Melt quenching was used in the preparation process. The samples melted in a porcelain melting-pot at 300°C for half an hour and then at 1000°C for an hour in an electric muffle furnace (LENTON) and it immediately poured between two copper plates.

The samples were examined using Philips Analytical X-ray diffraction system, type PW3710 based on a Cu tube anode with a wavelength $\text{K}\alpha_1=1.5406$ oA and $\text{K}\alpha_2=1.54439$ oA. The step size was 0.05o, and the period per step was 2.5 seconds.

The density of the samples (ρ) is calculated using Archimedes principal method with toluene (99.99% purity) as an immersion liquid. The density of yield:

$$\rho = ((0.865 W_a))/(W_a - W_b) \text{ g cm}^{-3}$$

where W_a and W_b are the weight of samples in air and toluene respectively, and 0.865g cm^{-3} is the density of toluene at room temperature.

The Infrared spectrometer (type JASCO FTIR-4100, Japan) is used to detect the FTIR absorption spectra of the prepared samples at room temperature. Infrared spectrometer range is $2000\text{--}400\text{ cm}^{-1}$ with the aid of the KBr disc technique.

The optical absorption spectra range from 190 to 2500 nm using a computerized recording spectrophotometer (type JASCO, V-570).

The emission measurements were calculated by using the (JASCO-FP-6300) Spectrofluorometer in the (200–800 nm) wavelength range.

3. Results and discussion:

Fig. 1. shows the X-ray diffraction (XRD) patterns of prepared glass samples. It indicates all the studied samples are amorphous.

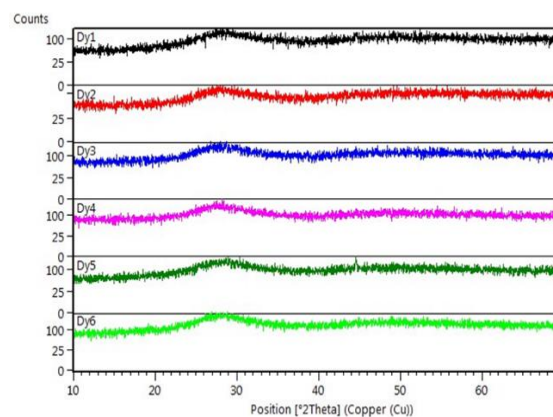


Fig. 1. X-ray diffraction (XRD) patterns of prepared glass samples

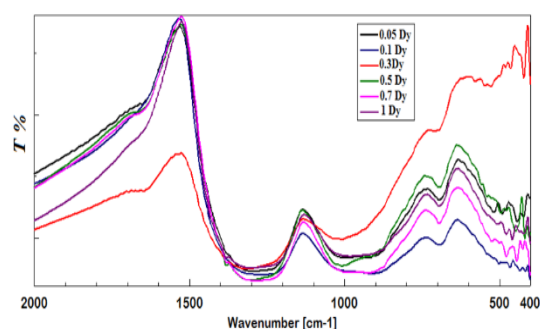


Fig. 2. FTIR of prepared glass samples

Fig. 2. shows the infrared spectra of glass samples doped with Dysprosium ions. From fig. 2, it could be noticed the band at 1636 cm^{-1} is due to the stretching vibration of the [OH] group [24]. Also, fig.2 observed

broad bands that indicate the overlapping of individual bands from B, Bi, and MO [11]. The stretching and bending vibration of borate groups are found in three regions [25]. Starting from the first region in the range 1200-1500 cm⁻¹ summarized the presence of the stretching of BO₃ with bridging and non-bridging types, the second in region 850-1200cm⁻¹ represented the stretching of the BO₄ group, and the last region in 600-800cm⁻¹ expressed the bending vibration of boron. The Bi and Mo in borate glass have a dual nature effect on the group formation and the linkage between different groups. Bismuth can be present as a former of the BiO₃ group [26] [27] at 848 cm⁻¹ and as a modifier of BiO₆ at 565 cm⁻¹ and 485 cm⁻¹. From fig 2, it observed the band at 450–530 cm⁻¹[28] appeared at 0.05 Dy and 0.3 Dy mol% glass samples assigned to the vibrations of Bi–O–Bi bonds in the octahedral [BiO₆]. The addition of MoO₃ to the glass network, results in the following equivalences of Mo⁶⁺ and Mo⁵⁺ or Mo⁴⁺. [25][29] form the tetrahedral MoO₄ and octahedral MoO₆ groups.

MoO₃ has two forms when added to glass: at low content, it acts as a network former, while at high content, it is a network modifier [25]. As the content of Mo is low (5 mol%), it probably acts as a former in the presence of samples. The bands of Mo were found at 835 and 890 cm⁻¹ and assigned to stretching vibrations of [MoO₄] anions [30][31][32]. A band at 880–870 cm⁻¹ represents MoO₆ octahedra [32] and a band around 600 and 450cm⁻¹ assigned to asymmetric and symmetric vibrations of Mo-O-Mo linkages [25]. It is observed that the band at ~415cm⁻¹ [26], which may be due to the vibration of alkali cations (Bi³⁺) or/and rare-earth ions (Dy³⁺).

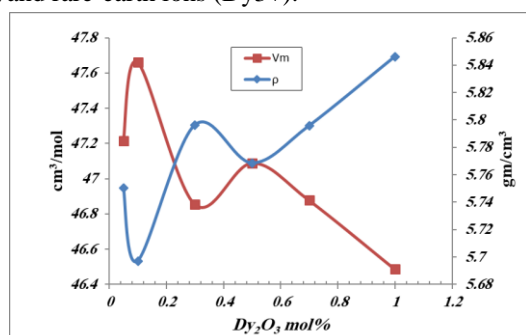


Fig.3. the relation between (density and molar volume) and the Dy₂O₃ concentration

Density and molar volume are the basis for studying the properties of the physical behavior of samples from the relationship between Density and molar volume as a function of Dy concentration shown in Fig.3. The

calculated areas of BO₃ and BO₄ obtained from the FTIR spectra deconvolution are shown in fig. 4.

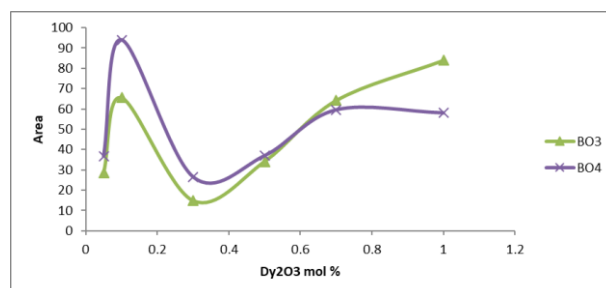


Fig.4 the relation between (area of BO₃ and BO₄) and the Dy₂O₃ concentration.

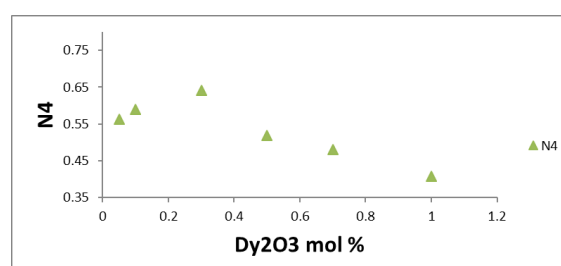


Fig. 5. Effect of Dy₂O₃ content on the N4 value

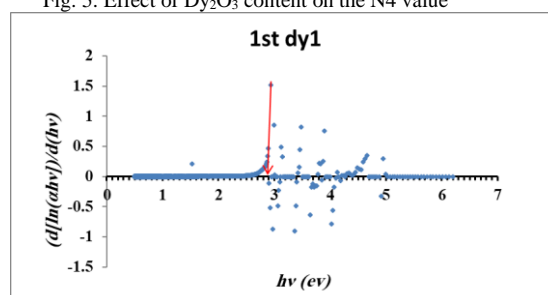


Fig.6 the differential method for Eg determination

The fraction of four-coordination boron atoms, N₄, is calculated to measure the relative changes in the BO₃ and BO₄ units shown in fig.5. From Fig. 3, it is observed that the density increases with increasing Dy concentration, it attributed to the molecular weight of Dy₂O₃[33][34], also doping the glass samples with Dy₂O₃ lead to increment the ratio of oxygen–boron in network and leading to a compact structure [27].

From fig. 4 observed the lowest values of BO₃ area, located at 0.05 and 0.3 Dy mol% points, which mean the conversion of some borate groups to BiO₆ group, and this agree with FTIR analysis.

Optical band gap is the energy required by photons to excite the electrons from the valence band to the conduction band. It derived from the derivative method according to the relation: [35]

$$\frac{d[\ln(\alpha h\nu)]}{d(h\nu)} = \frac{n}{h\nu - E_{opt}}$$

Where α is the absorption coefficient, h is planck's constant, ν is the frequency, n is the refractive index and E_{opt} is the optical bandgap energy.

The obtained value observed in table.3 indicate the decrease of the E_{opt} value with adding Dy as the increase of Dy perform the electron localization tending to increase in the doner center [36][8]. This value is identical with other researchers [33][37] and is in agreement with the molar volume trend.

Table 1. various IR peaks observed in the glass systems.

Dy % samples	IR band positions Wave number(cm-1)						
0.05	1442	1340	1210	1059	914	730	
0.1	1440	1324	1205	1068	917	714	
0.3	1425	1360	1301	1222	1046	886	
0.5	1428	1314	1206	1045	896	779	
0.7	1416	1294	1198	1061	911	737	
1	1428	1306	1198	1064	921	771	

Table 2. Vibration types of different IR wave numbers

IR band positions Wave number(cm-1)	Assignments
1200–1500 cm ⁻¹	Asymmetric stretching BO bond of [BO3] groups
1406–1490 cm ⁻¹	are assigned to the asymmetrical stretching vibrations with three NBOs of the B-O-B groups
850-1200	Stretching vibration of B-O-B linkage of tetrahedral BO4 units
848 cm-1 565 and 485 cm-1 <650 cm-1	BiO3 former BiO6 modifier may be due to the bond bending vibrations of Bi=O bonds in BiO6 octahedral units and BiO3 pyramidal units
450–530 cm ⁻¹	assigned to the vibrations of Bi–O–Bi bonds in the octahedral [BiO6]
~ 415cm-1	may due to the vibration of alkali cation(Bi+3) or/and rare earth ions (Dy3+)
835 & 870 cm-1 880-870 cm-1 600 cm-1 450 cm-1	stretching vibrations of [MoO4] anions MoO6 octahedra Asymmetric vibrations of Mo-O-Mo symmetric vibrations of Mo-O-Mo

Table.3. Some Physical and optical parameters of the glass samples for different Dy₂O₃ contents

Dymol%	E _g eV	n	R _L	T	χ ³ *10 ⁻¹² e.s.u	χ ¹	R _m	M	am=Rm/2.52
0.05	2.90	2.424	0.173	0.704	2.27	0.388	30.26	0.380	12.01
0.1	2.95	2.410	0.171	0.707	2.15	0.383	30.44	0.384	12.07
0.3	2.93	2.416	0.171	0.706	2.20	0.385	30.33	0.382	12.035
0.5	2.93	2.416	0.171	0.706	2.20	0.385	29.91	0.382	11.86
0.7	2.93	2.416	0.171	0.706	2.20	0.385	31.58	0.382	12.53
1	2.93	2.416	0.171	0.706	2.20	0.385	29.65	0.382	11.76

By using the optical bandgap, the refractive index of samples using the following relation:

$$\frac{n^2 - 1}{n^2 + 2} = 1 - \sqrt{\frac{E_{opt}}{20}}$$

In continuous reflection (RL), transmission (T) and the third-order nonlinear susceptibility χ⁽³⁾

parameters determined according to the following relations [38]

$$R_L = \left[\frac{n-1}{n+1} \right]^2 \quad T = \frac{2n}{n^2+1} \quad \text{And} \\ \chi^{(3)} = [\chi^{(1)}]^4 \times 10^{-10}$$

where χ⁽¹⁾ is the linear optical susceptibility calculated as

$$\chi^{(1)} = \frac{(n^2 - 1)}{4\pi}$$

The total polarizability of material per mole through Lorenz-Lorenz equation from the relation [39]

$$R_m = [(n_0^2 - 1)/(n_0^2 + 2)]V_m$$

The metallization [40] is an important value that determined the nature of bonding in each glass sample according to the relation

$$M = 1 - \frac{R_m}{V_m}$$

The magnitude of electron cloud deformation under the application of electromagnetic wave arising from the presence of oxygen in glass with different shapes as bridging, non-bridging, or negative charge called Electronic polarizability [38][39][41] calculated according to the following relation

$$\alpha_m = \left(\frac{3}{4\pi N_A}\right)R_m$$

Where α_m is electronic polarizability, N_A represents the Avogadro's number. The obtained values are tabulated in table 3, from table many physical properties are explained, as the values of $X^{(3)}$ which indicate the availability of using glass in nonlinear optical applications, the values of metallization is less than unity and constant as the nonmetallic bond [42], at constant concentration of bismuth oxide, the importance of prepared glass in using as nonlinear optical application[38]

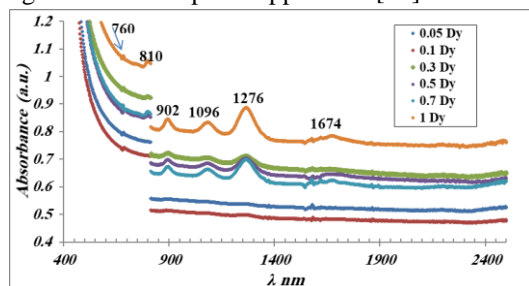


Fig. 7. UV-Vis optical absorption spectra of glasses with different Dy₂O₃ contents.

Fig. 7. shows the optical absorption of samples under study exhibited the following resolved peaks [18][21] 6H15/2→6H11/2 (1688nm), 6F11/2+6H9/2(1274nm), 6F9/2+6H7/2 (1090nm), 6F7/2 (900nm), 6F5/2 (806nm) and 6F3/2 (758nm). The intensity of the absorption peaks increases without any significant shift in the peak position. The oscillator strengths in the experimental method determined according to the relation [21]

$$f_{exp} = 4.318 \times 10^{-9} \int \alpha(\nu) d\nu$$

The oscillator strength could be determined theoretically according to the relation [21]

$$f_{cal} = \frac{8\pi^2 mc(n^2+1)^2}{3h\lambda(2J+1)9n} \sum_{\lambda=2,4,6} \Omega_{\lambda}(\Psi) \|U^{\lambda}\| \langle \psi' | J' \rangle^2$$

Where ν is the wavenumber (cm⁻¹) of the excitation from ground state(ψJ) to the excited state ($\psi' J'$), c is the velocity of light in vacuum; m is the rest mass of an electron and $\|U^{\lambda}\|^2$ doubly reduced matrix element.

The fit quality between the obtained F_{cal} and F_{exp} values (in table4) determine from the root-mean-square deviation based on the following equation:

$$\delta_{rms} = \left[\frac{\sum (f_{exp} - f_{cal})^2}{N-3} \right]^{1/2} \quad (5)$$

Where N is the total number of the energy levels used in the fit.

The lowest values of δ_{rms} ranged from 10-6 give the high quality and validity of JO analysis. Judd-Ofelt parameters Ω_2 , Ω_4 , and Ω_6 are interesting for investigating the local structure in a glass matrix around a rare-earth ion. From the obtained parameters, Ω_2 has a higher value than Ω_4 , and Ω_6 indicates the higher covalency and asymmetry around Dy³⁺ [18].

Many researchers studied the bismuth borate glass containing Dy ions and found the position of Dy in an asymmetric site with a weak bond with oxygen surrounding it [43][44][45][46][47].

Judd-Ofelt parameters are beneficial in predicting the relaxation of Dy from the metastable level 4F9/2 formed laser emission determined by the ratio Ω_4/Ω_6 [43][45][46]. From the value of Ω_4/Ω_6 in table 4 it is observed that the values increase with the increase of Dy concentration to reach a maximum value 1.2 at 1 Dy mol%, predicting the ability of material for the laser emission.

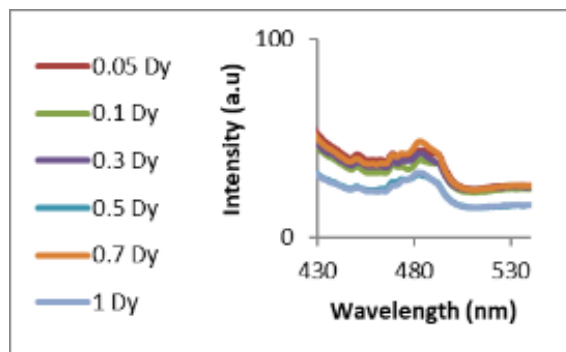


Fig. 8. illustrates the excitation spectra of the high concentration glass sample with 1mol% Dy by monitoring emission at 575nm. It is observed that the six bands[48][20][49] at 352, 367, 384, 429, 454, and 476nm represented the excitation from the 6H15/2 (ground level) to 6P7/2, 6P5/2, 4I13/2, 4G11/2, 4I13/2 and 4F9/2 (an excited level) respectively, with high intensity located at 384 nm, in accordance with the literature [50][51] [52].

Table 4. Experimental and calculated oscillator strengths for Dy³⁺-doped glass

λnm	1Dy%		0.7Dy%		0.5Dy%		0.3Dy%	
	f _{exp}	f _{cal}						
1674	6.71	6.62	8.80	7.67	12	9.43	5.73	5.07
1276	44.8	47.8	42.8	45.8	50	53.7	27.5	29.3
1096	11.4	11.9	14	14.2	13.5	13	7.05	7.07
902	7.74	8.96	8.25	11.6	7.68	13	4.96	6.94
810	2.94	3.94	3.15	5.33	1.22	6.53	2.06	3.48
758	0.31	0.74	0.26	1	0.42	1.23	---	---
Δrms	3.51		4.83		6.97		3.27	
Ω4/Ω26	1.20E+00		9.08E-01		3.67E-01		3.96E-01	

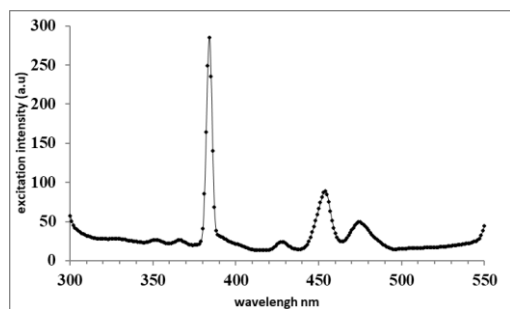


Fig. 8. the excitation spectra of glass sample with 1mol% Dy.

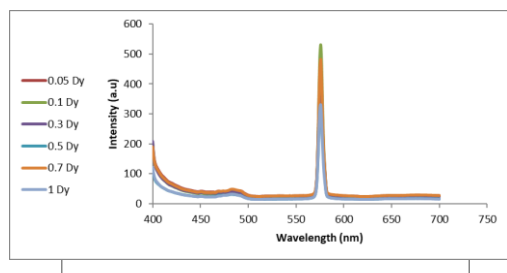
Fig 9. Emission spectra of glasses with different Dy₂O₃ contents excitation energy at 450 nm

Fig. 9. shows the emission of glass samples doped with Dy³⁺ excited at 384nm. From fig 7, it could be observed that the three emission bands.[21][53] at 485nm (4F_{9/2} → 6H_{15/2}) represents the blue emission and it has a magnetic dipole transition which is less efficient with the composition system. The band at 575-584nm (4F_{9/2} → 6H_{13/2}) represents the yellow emission. It has electric dipole transition that is affected by the glass surrounding it and at 650nm (6H_{11/2}) represents the red emission. From figx observed the transition 4F_{9/2} → 6H_{15/2} is relatively quite weak, and 4F_{9/2} → 6H_{13/2} transition is hypersensitive. The 4F_{9/2} → 6H_{13/2} transition is heavily affected by the environment around the Dy³⁺-ion site, referring to the lower symmetry around the Dy³⁺ ions sites as well as the higher covalency between Dy and oxygen ligand[54][52][55]. The ratio between the electric and the magnetic dipoles [56]

determining the efficiency of the white LED and the symmetry around Dy. The higher Y/B illustrates the asymmetric ligand environment [50]. From the Y/B values in table 5, the Y/B ratio increased with the Dy concentration increment up to 0.5 mol% to reach the maximum value and then decrease, which could explain the possibility of white light emission [57].

The color is a result of the ratio of the primary color[25] is beneficial in a determination by 2 points by CIE 1931 chromaticity. The measured points produced in the emission spectra and the CIE 1931 chromaticity determine the (x, y) points for each glass sample excited at 384nm shown in fig. 10. From fig. 10., the values extracted from the CIE 1931 chromaticity tabulate in table 5. The results obtained in the table and with the aid of fig.10 are observed the higher values of x,y chromaticity that represent the prepared glass samples ranged in the white region. The two-point produced by CIE 1931 chromaticity[14][19] [25] reduced to one point with the introduction of the Correlated Color Temperature (CCT). CCT important light characterization as Today the light, it is classified as the cool light used in many places such as schools, offices, and hospitals, or the warm light used in houses and restaurants. CCT determined by the following relation

$$CCT = -449n^3 + 352n^2 - 6823n + 5520.33$$

$$\text{Where } n = (x-0.332)/(y-0.186)$$

and CCT

$$n = \frac{x - 0.332}{y - 0.186}$$

With the help of Judd Ofelt parameters which obtained from the absorption spectra, it can predict the radiative parameter as the transition probability from the ground state to the excited state according to the relation[58]

$$A = \frac{64\pi^4\nu^3}{3h(2J+1)} \left[\frac{\eta(n^2+2)^2}{9n} S_{ed} \right]$$

Where n is the refractive index, n is the energy of the

transition (cm⁻¹), S_{ed} is the electric-dipole line strength and calculated according to the following relation.

$$S_{ed} = e^2 \sum_{\lambda=2,4,6} \Omega_{\lambda} \|U^{\lambda}\|^2$$

In which Ω_{λ} is the JO parameters, and $\|U^{\lambda}\|$ is the double squares reduced unit tensor operators for the luminescence states

The total transition probability of emission level is given by [58]:

$$A_T = \sum A$$

The predicted radiative lifetime (TR) [50] given by

$$\tau_R = [A_T(\Psi)]^{-1}$$

The luminescence branching ratio (β_R)

[59] corresponding to the emission from the excited level (4F_{9/2}) to a lower level that characterizes the lasing power of the potential laser transitions from the relation and it calculated as the emission transition having a luminescence branching ratio (β_R) greater than 50% [49] is considered to have more potential for laser emission

$$\beta_R = \frac{A_R(\Psi, \Psi')}{A_T(\Psi)}$$

And can be calculated experimentally from the intensities of emission bands.

The integrated absorption cross-section, σ_a [58], for the stimulated emission for a fluorescent level is given by

$$\sigma_a = \frac{1}{\nu^2} \frac{A}{8\pi c n^2}$$

All the values are calculated and tabulated in table 6.

Table 5 . J-O Intensity parameters, Y/B ratio, (X,Y) chromaticity

Dymol%	0.05	0.1	0.3	0.5	0.7	1
$\Omega_{\lambda} * 10^{-20}$	----	-----	$\Omega_2=28.3$ $\Omega_4=2.59$ $\Omega_6=6.54$	$\Omega_2= 52$ $\Omega_4=4.5$ $\Omega_6=12.3$	$\Omega_2= 39.8$ $\Omega_4=9.09$ $\Omega_6=10.01$	$\Omega_2=42.7$ $\Omega_4= 8.87$ $\Omega_6= 7.39$
Y/B	6.482363	7.431295	4.702516	5.072605	4.702516	4.961579
(X,y) chromaticity	(0.327,0.321)	(0.329,0.331)	(0.318,0.318)	(0.317,0.31)	(0.33,0.32)	(0.323, 0.319)
CCT	5753	5652	6240	6255	5525	5966

Table 6 The radiative life time and branching ratio calculations

Dyconc%	A	AT= $\sum A$	BR calc	TR=[AT] ⁻¹	$\sigma=A/(8\pi c n^2) \nu^2$	
0.3	485	188.5	1170.3	16.108	854.4886	1.0081E-19
	576	981.8		83.892		7.4051E-19
0.5	485	352.6	2161.6	16.311	462.6273	1.88551E-19
	576	1809.0		83.689		1.36443E-18
0.7	485	303.4	1758.3	17.253	568.7400	1.6223E-19
	576	1454.9		82.747		1.09737E-18
1	485	230.1	1681.5	13.685	594.6912	1.23064E-19
	576	1451.4		86.315		1.09474E-18

From table 6, it is observed that the branching ratio calculated from Judd Ofelt is analogous to the values obtained from experimental results for yellow transition and has a higher value than blue emission that the relatively larger Bcal values and stimulated

emission cross-sections are observed the values decrease with the increase of Dy concentrations; making them promising materials for lasing action [43] through the emission channel 4F_{9/2}-6H_{13/2} with a wavelength around 576 nm.

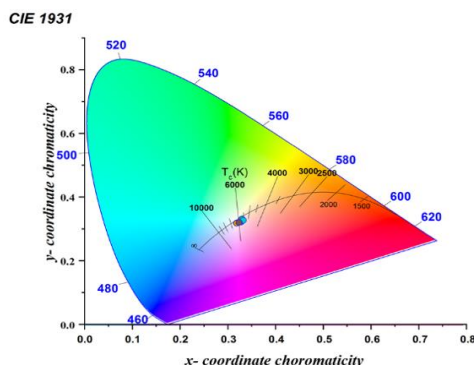


Fig. 10. The color coordination of glass samples doped with Dy excited 450nm

4. Conclusions

A glass of molybdenum-bismuth borate containing dysprosium ions was prepared. The glassy nature of the behavior of samples is confirmed using the XRD spectrum. The amorphous nature was determined from the first sight of glass samples that it appeared clear and confirmed with XRD measurement. The vibration Agroups related to molybdenum bismuth borate glasses is determined using the FT-IR technique. The highest values of Ω_2 represent covalent bonding nature. The branching ratios and emission cross-sectional values reveal the availability of the glass samples understudy for the applications of yellow laser. The obtained results are reliable with the CIE chromaticity coordinates and the Y/B ratio.

5. References:

- [1] L. Mishra et al., "White light emission and color tunability of dysprosium doped barium silicate glasses," *J. Lumin.*, vol. 169, pp. 121–127, 2016, doi: 10.1016/j.jlumin.2015.08.063.
- [2] Y. Zhou, D. Chen, W. Tian, and Z. Ji, "Impact of Eu^{3+} dopants on optical spectroscopy of $\text{Ce}^{3+}:\text{Y}_3\text{Al}_5\text{O}_{12}$ -embedded transparent glass-ceramics," *J. Am. Ceram. Soc.*, vol. 98, no. 8, pp. 2445–2450, 2015.
- [3] T. Emission, P. Ca, and E. Transfer, "Panlai Li, † Zhijun Wang, † Qinglin Guo, and Zhiping Yang," vol. 500, no. 35296, pp. 3–8, 2015, doi: 10.1111/jace.13292.
- [4] R. Ye et al., "Luminescence and energy transfer of $\text{Eu}^{2+}/\text{Mn}^{2+}$ co-doped $\text{SiO}_2 - \text{Al}_2\text{O}_3 - \text{ZnO} - \text{K}_2\text{O}$ glass ceramics for white LEDs," vol. 130, pp. 2385–2389, 2010, doi: 10.1016/j.jlumin.2010.07.023.
- [5] T. Glass-ceramics, "Yang Zhou, Daqin Chen, † Wendong Tian, and Zhenguo Ji," vol. 2450, no. 36391, 2015, doi: 10.1111/jace.13668.
- [6] L. Ren, X. Lei, X. Du, L. Jin, W. Chen, and Y. Feng, "Effect of Eu_2O_3 concentration on luminescent properties of $\text{Ce} / \text{Tb} / \text{Eu} \dot{\text{C}}$ co-doped calcium borosilicate glass for white LED," vol. 142, pp. 150–154, 2013.
- [7] C. Zhu, D. Wu, J. Liu, M. Zhang, and Y. Zhang, "Color-tunable luminescence in Ce -, Dy -, and Eu -doped oxyfluoride aluminoborosilicate glasses," *J. Lumin.*, vol. 183, pp. 32–38, 2017, doi: 10.1016/j.jlumin.2016.11.004.
- [8] P. P. Pawar, S. R. Munishwar, S. Gautam, and R. S. Gedam, "Physical, thermal, structural and optical properties of Dy^{3+} doped lithium alumino-borate glasses for bright W-LED," *J. Lumin.*, vol. 183, pp. 79–88, 2017, doi: 10.1016/j.jlumin.2016.11.027.
- [9] P. Chimalawong, K. Kirdsiri, J. Kaewkhao, and P. Limsuwan, "Investigation on the Physical and Optical Properties of Dy^{3+} Doped Soda-Lime-Silicate Glasses," *Procedia Eng.*, vol. 32, pp. 690–698, 2012, doi: 10.1016/j.proeng.2012.01.1328.
- [10] Y. Wei et al., "Luminescence and preparation of Dy_2O_3 doped $\text{SrCO}_3 - \text{WO}_3 - \text{SiO}_2$ glass ceramics," *J. Lumin.*, vol. 220, no. August 2019, 2020, doi: 10.1016/j.jlumin.2019.117021.
- [11] K. S. Shaaban, A. A. El-Maaref, M. Abdelawwad, Y. B. Saddeek, H. Wilke, and H. Hillmer, "Spectroscopic properties and Judd-Ofelt analysis of Dy^{3+} ions in molybdenum borosilicate glasses," *J. Lumin.*, vol. 196, no. May 2017, pp. 477–484, 2018, doi: 10.1016/j.jlumin.2017.12.041.
- [12] A. A. El-Maaref, K. S. Shaaban, M. Abdelawwad, and Y. B. Saddeek, "Optical characterizations and Judd-Ofelt analysis of Dy^{3+} doped borosilicate glasses," *Opt. Mater. (Amst.)*, vol. 72, pp. 169–176, 2017, doi: 10.1016/j.optmat.2017.05.062.
- [13] S. Peng et al., "A novel type of borosilicate glass with excellent chemical stability and high ultraviolet transmission," *J. Non. Cryst. Solids*, vol. 528, no. October 2019, pp. 1–6, 2020, doi: 10.1016/j.jnoncrysol.2019.119735.
- [14] V. P. Tuyen et al., "An in-depth study of the Judd-Ofelt analysis, spectroscopic properties and

- energy transfer of Dy 3+ in aluminio-lithium-telluroborate glasses,” *J. Lumin.*, vol. 210, no. November 2018, pp. 435–443, 2019, doi: 10.1016/j.jlumin.2019.03.009.
- [15] P. Van Do et al., “Energy transfer phenomena and Judd-Ofelt analysis on Sm 3+ ions in K 2 GdF 5 crystal,” *J. Lumin.*, vol. 179, pp. 93–99, 2016, doi: 10.1016/j.jlumin.2016.06.051.
- [16] S. A. Azizan, S. Hashim, N. A. Razak, M. H. A. Mhareb, Y. S. M. Alajerami, and N. Tamchek, “Physical and optical properties of Dy³⁺: Li₂O-K₂O-B₂O₃ glasses,” *J. Mol. Struct.*, vol. 1076, pp. 20–25, 2014, doi: 10.1016/j.molstruc.2014.07.032.
- [17] C. K. Jayasankar, V. Venkatramu, S. S. Babu, and P. Babu, “Luminescence properties of Dy³⁺ ions in a variety of borate and fluoroborate glasses containing lithium, zinc, and lead,” *J. Alloys Compd.*, vol. 374, no. 1–2, pp. 22–26, 2004, doi: 10.1016/j.jallcom.2003.11.051.
- [18] A. Balakrishna, D. Rajesh, and Y. C. Ratnakaram, “Structural and photoluminescence properties of Dy³⁺ doped different modifier oxide-based lithium borate glasses,” *J. Lumin.*, vol. 132, no. 11, pp. 2984–2991, 2012, doi: 10.1016/j.jlumin.2012.06.014.
- [19] S. Kaur et al., “Blue-yellow emission adjustability with aluminium incorporation for cool to warm white light generation in dysprosium doped borate glasses,” *J. Lumin.*, vol. 202, no. May, pp. 168–175, 2018, doi: 10.1016/j.jlumin.2018.05.034.
- [20] K. V. Rao, S. Babu, G. Venkataiah, and Y. C. Ratnakaram, “Optical spectroscopy of Dy 3 + doped borate glasses for luminescence applications,” *J. Mol. Struct.*, vol. 1094, no. April, pp. 274–280, 2015, doi: 10.1016/j.molstruc.2015.04.015.
- [21] V. Uma, K. Maheshvaran, K. Marimuthu, and G. Muralidharan, “Structural and optical investigations on Dy³⁺ doped lithium tellurofluoroborate glasses for white light applications,” *J. Lumin.*, vol. 176, pp. 15–24, 2016, doi: 10.1016/j.jlumin.2016.03.016.
- [22] D. D. Ramteke, R. S. Gedam, and H. C. Swart, “Physical and optical properties of lithium borosilicate glasses doped with Dy³⁺ ions,” *Phys. B Condens. Matter*, vol. 535, no. April 2017, pp. 194–197, 2018, doi: 10.1016/j.physb.2017.07.035.
- [23] X. Sun, S. Huang, Q. Gao, Z. Ye, C. Cao, and others, “Spectroscopic properties and simulation of white-light in Dy³⁺-doped silicate glass,” *J. Non. Cryst. Solids*, vol. 356, no. 2, pp. 98–101, 2010.
- [24] L. Xia, L. Wang, Q. Xiao, Z. Li, W. You, and Q. Zhang, “Preparation and luminescence properties of Eu³⁺ doped calcium bismuth borate red-light-emitting glasses for WLEDs,” *J. Non. Cryst. Solids*, vol. 476, no. September, pp. 151–157, 2017, doi: 10.1016/j.jnoncrysol.2017.09.049.
- [25] S. M. Abo-Naf, “FTIR and UV-VIS optical absorption spectra of gamma-irradiated MoO 3-doped lead borate glasses,” *J. Non. Cryst. Solids*, vol. 358, no. 2, pp. 406–413, 2012, doi: 10.1016/j.jnoncrysol.2011.10.013.
- [26] P. Narwal, M. S. Dahiya, A. Yadav, A. Hooda, A. Agarwal, and S. Khasa, “Improved white light emission in Dy 3+ doped LiF–CaO–Bi 2 O 3 –B 2 O 3 glasses,” *J. Non. Cryst. Solids*, vol. 498, no. November 2017, pp. 470–479, 2018, doi: 10.1016/j.jnoncrysol.2018.01.042.
- [27] Q. Chen, M. Zhang, Q. Ma, and Q. Wang, “The structure, spectra and properties of Dy₂O₃ modified diamagnetic lead-bismuth-germanium glasses,” *J. Non. Cryst. Solids*, vol. 507, no. December 2018, pp. 46–55, 2019, doi: 10.1016/j.jnoncrysol.2018.09.025.
- [28] N. M. Bobkova, S. A. Artem’eva, and E. E. Trusova, “Behavior of copper oxide in silicoborate glazed glasses,” *Glas. Ceram. (English Transl. Steklo i Keramika)*, vol. 64, no. 7–8, pp. 264–266, 2007, doi: 10.1007/s10717-007-0065-9.
- [29] M. I. Sayyed, K. M. Kaky, D. K. Gaikwad, O. Agar, U. P. Gawai, and S. O. Baki, “Physical, structural, optical and gamma radiation shielding properties of borate glasses containing heavy metals (Bi 2 O 3 /MoO 3),” *J. Non. Cryst. Solids*, vol. 507, no. December 2018, pp. 30–37, 2019, doi: 10.1016/j.jnoncrysol.2018.12.010.
- [30] P. S. Prasad, B. V. Raghavaiah, R. Balaji Rao, C. Laxmikanth, and N. Veeraiah, “Dielectric dispersion in the PbO–MoO₃–B₂O₃ glass system,” *Solid State Commun.*, vol. 132, no. 3–4, pp. 235–240, 2004, doi: 10.1016/j.ssc.2004.07.042.
- [31] N. Rajya Lakshmi and S. Cole, “Influence of MoO₃ ions on spectroscopic properties of B₂O₃–ZnF₂–CaF₂–Al₂O₃ oxyfluoride glasses,” *Mater. Today Proc.*, vol. 5, no. 13, pp. 26346–26355, 2018, doi: 10.1016/j.matpr.2018.08.086.
- [32] L. Aleksandrov, R. Iordanova, and Y. Dimitriev, “Glass formation in the MoO₃–Nd₂O₃–La₂O₃–B₂O₃ system,” *J. Non. Cryst. Solids*, vol. 355, no. 37–42, pp. 2023–2026, 2009, doi: 10.1016/j.jnoncrysol.2009.05.069.
- [33] I. Khan et al., “Photoluminescence and white light generation of Dy₂O₃ doped Li₂O–BaO–Gd₂O₃–SiO₂ for white light LED,” *J. Alloys Compd.*, vol. 774, pp. 244–254, 2019, doi: 10.1016/j.jallcom.2018.09.156.
- [34] M. Monisha, N. Mazumder, G. Lakshminarayana, S. Mandal, and S. D. Kamath, “Energy transfer and luminescence study of Dy³⁺ doped zinc-aluminoborosilicate glasses for white light

- emission,” *Ceram. Int.*, no. June, pp. 1–13, 2020, doi: 10.1016/j.ceramint.2020.08.167.
- [35] I. Kashif and A. Ratep, “Effect of copper addition on BO₄, H₂O groups and optical properties of lithium lead borate glass,” *Opt. Quantum Electron.*, vol. 49, no. 6, 2017, doi: 10.1007/s11082-017-1067-7.
- [36] P. Gayathri Pavani, K. Sadhana, and V. Chandra Mouli, “Optical, physical and structural studies of boro-zinc tellurite glasses,” *Phys. B Condens. Matter*, vol. 406, no. 6–7, pp. 1242–1247, 2011, doi: 10.1016/j.physb.2011.01.006.
- [37] Y. Saleh et al., “Optical properties of lithium magnesium borate glasses doped with Dy³⁺ and Sm³⁺ ions,” *Phys. B Phys. Condens. Matter*, vol. 407, no. 13, pp. 2398–2403, 2012, doi: 10.1016/j.physb.2012.03.033.
- [38] I. K. A. Ratep and G. Adel, “Polarizability, optical basicity and optical properties,” *Applied Physics A*, vol. 0, no. 0, p. 0, 2018, doi: 10.1007/s00339-018-1904-y.
- [39] M. K. Halimah, M. F. Faznny, M. N. Azlan, and H. A. A. Sidek, “Optical basicity and electronic polarizability of zinc borotellurite glass doped La³⁺ ions,” *Results Phys.*, vol. 7, pp. 581–589, 2017, doi: 10.1016/j.rinp.2017.01.014.
- [40] S. H. Alazoumi et al., “Optical properties of zinc lead tellurite glasses,” *Results Phys.*, vol. 9, no. April, pp. 1371–1376, 2018, doi: 10.1016/j.rinp.2018.04.041.
- [41] A. Edukondalu et al., “Mixed alkali effect in physical and optical properties of Li₂O–Na₂O–WO₃–B₂O₃ glasses,” *J. Non. Cryst. Solids*, vol. 358, no. 18–19, pp. 2581–2588, 2012, doi: 10.1016/j.jnoncrsol.2012.06.004.
- [42] T. Honma, R. Sato, Y. Benino, T. Komatsu, and V. Dimitrov, “Electronic polarizability, optical basicity and XPS spectra of Sb₂O₃–B₂O₃ glasses,” *J. Non. Cryst. Solids*, vol. 272, no. 1, pp. 1–13, 2000.
- [43] K. Swapna, S. Mahamuda, A. Srinivasa Rao, M. Jayasimhadri, T. Sasikala, and L. Rama Moorthy, “Optical absorption and luminescence characteristics of Dy³⁺ doped Zinc Alumino Bismuth Borate glasses for lasing materials and white LEDs,” *J. Lumin.*, vol. 139, pp. 119–124, 2013, doi: 10.1016/j.jlumin.2013.02.035.
- [44] B. Shanmugavelu and V. V. R. K. Kumar, “Luminescence studies of Dy³⁺ doped bismuth zinc borate glasses,” *J. Lumin.*, vol. 146, pp. 358–363, 2014, doi: 10.1016/j.jlumin.2013.10.018.
- [45] K. Swapna, S. Mahamuda, A. Srinivasa Rao, M. Jayasimhadri, T. Sasikala, and L. Rama Moorthy, “Visible fluorescence characteristics of Dy³⁺ doped zinc alumino bismuth borate glasses for optoelectronic devices,” *Ceram. Int.*, vol. 39, no. 7, pp. 8459–8465, 2013, doi: 10.1016/j.ceramint.2013.04.028.
- [46] M. Mariyappan, S. Arunkumar, and K. Marimuthu, “White light emission and spectroscopic properties of Dy³⁺ ions doped bismuth sodiumfluoroborate glasses for photonic applications,” *J. Alloys Compd.*, vol. 723, pp. 100–114, 2017, doi: 10.1016/j.jallcom.2017.06.244.
- [47] H. Zhang, P. J. Lin, J. L. Yuan, E. Y. B. Pun, D. S. Li, and H. Lin, “Multiplier effect of sensitization for Dy³⁺ fluorescence in borosilicate glass phosphor,” *J. Lumin.*, vol. 221, no. September, 2019, 2020, doi: 10.1016/j.jlumin.2020.117062.
- [48] A. Ichoja, S. Hashim, S. K. Ghoshal, and I. H. Hashim, “Absorption and luminescence spectral analysis of Dy³⁺-doped magnesium borate glass,” *Chinese J. Phys.*, vol. 66, no. March, pp. 307–317, 2020, doi: 10.1016/j.cjph.2020.03.029.
- [49] K. Vijaya Babu and S. Cole, “Luminescence properties of Dy³⁺-doped alkali lead alumino borosilicate glasses,” *Ceram. Int.*, vol. 44, no. 8, pp. 9080–9090, 2018, doi: 10.1016/j.ceramint.2018.02.115.
- [50] M. V. Rao, B. Shanmugavelu, and V. V. R. K. Kumar, “Optical absorption and photoluminescence studies of Dy³⁺ doped alkaline earth bismuth borate glasses,” *J. Lumin.*, vol. 181, pp. 291–298, 2017, doi: 10.1016/j.jlumin.2016.09.012.
- [51] Y. Ma et al., “Structural characterization and photoluminescence properties of B₂O₃–Bi₂O₃–SiO₂ glass containing Dy³⁺ ions,” *J. Lumin.*, vol. 227, p. 117591, 2020.
- [52] Y. A. Lakshmi, K. Swapna, K. S. R. K. Reddy, S. Mahamuda, M. Venkateswarulu, and A. S. Rao, “Concentration dependent photoluminescence studies of Dy³⁺ doped Bismuth Boro-Tellurite glasses for lasers and wLEDs,” *Opt. Mater. (Amst.)*, vol. 109, p. 110328, 2020.
- [53] S. Selvi, G. Venkataiah, S. Arunkumar, G. Muralidharan, and K. Marimuthu, “Structural and luminescence studies on Dy³⁺ doped lead borotelluro-phosphate glasses,” *Phys. B Condens. Matter*, vol. 454, pp. 72–81, 2014, doi: 10.1016/j.physb.2014.07.018.
- [54] G. Lakshminarayana et al., “Dy³⁺: B₂O₃–Al₂O₃–ZnF₂–NaF/LiF oxyfluoride glasses for cool white or day white light-emitting applications,” *Opt. Mater. (Amst.)*, vol. 108, no. July, p. 110186, 2020, doi: 10.1016/j.optmat.2020.110186.
- [55] P. R. Rani, M. Venkateswarlu, S. Mahamuda, K. Swapna, N. Deopa, and A. S. Rao, “Spectroscopic studies of Dy³⁺ ions doped barium lead alumino

- fluoro borate glasses,” *J. Alloys Compd.*, vol. 787, pp. 503–518, 2019.
- [56] S. Arunkumar and K. Marimuthu, “Concentration effect of Sm³⁺ ions in B₂O₃-PbO-PbF₂-Bi₂O₃-ZnO glasses - Structural and luminescence investigations,” *J. Alloys Compd.*, vol. 565, pp. 104–114, 2013, doi: 10.1016/j.jallcom.2013.02.151.
- [57] P. Narwal, M. S. Dahiya, A. Yadav, A. Hooda, A. Agarwal, and S. Khasa, “Improved white light emission in Dy³⁺ doped LiF-CaO-Bi₂O₃-B₂O₃ glasses,” *J. Non. Cryst. Solids*, vol. 498, no. January, pp. 470–479, 2018, doi: 10.1016/j.jnoncrysol.2018.01.042.
- [58] A. Srinivasa Rao et al., “Spectroscopic and optical properties of Nd³⁺ doped fluorine containing alkali and alkaline earth zinc-aluminophosphate optical glasses,” *Phys. B Condens. Matter*, vol. 404, no. 20, pp. 3717–3721, 2009, doi: 10.1016/j.physb.2009.06.114.
- [59] V. Himamaheswara Rao et al., “Spectroscopic studies of Dy³⁺ ion doped tellurite glasses for solid state lasers and white LEDs,” *Spectrochim. Acta - Part A Mol. Biomol. Spectrosc.*, vol. 188, pp. 516–524, 2018, doi: 10.1016/j.saa.2017.07.013.